Quaternary Science Reviews 155 (2017) 1–12

Contents lists available at ScienceDirect

Quaternary Science Reviews

journal homepage: www.elsevier.com/locate/quascirev

Invited review

# A paleo-perspective on ocean heat content: Lessons from the Holocene and Common Era

Yair Rosenthal [a,*], Julie Kalansky [b], Audrey Morley [c], Braddock Linsley [d]

[a] Department of Marine and Coastal Science and Department of Earth and Planetary Sciences, Rutgers University, USA
[b] Scripps Institution of Oceanography, University of California San Diego, USA
[c] School of Geography and Archaeology, National University of Ireland Galway, Galway, Ireland
[d] Lamont-Doherty Earth Observatory of Columbia University, New York, NY, USA

ARTICLE INFO

*Article history:*
Received 15 April 2016
Received in revised form
13 October 2016
Accepted 28 October 2016
Available online 12 November 2016

*Keywords:*
Ocean heat content (OHC)
Coral
Holocene
Mg/Ca
Foraminifera

ABSTRACT

The ocean constitutes the largest heat reservoir in the Earth's energy budget and thus exerts a major influence on its climate. Instrumental observations show an increase in ocean heat content (OHC) associated with the increase in greenhouse emissions. Here we review proxy records of intermediate water temperatures from sediment cores and corals in the equatorial Pacific and northeastern Atlantic Oceans, spanning 10,000 years beyond the instrumental record. These records suggests that intermediate waters were 1.5–2 °C warmer during the Holocene Thermal Maximum than in the last century. Intermediate water masses cooled by 0.9 °C from the Medieval Climate Anomaly to the Little Ice Age. These changes are significantly larger than the temperature anomalies documented in the instrumental record. The implied large perturbations in OHC and Earth's energy budget are at odds with very small radiative forcing anomalies throughout the Holocene and Common Era. We suggest that even very small radiative perturbations can change the latitudinal temperature gradient and strongly affect prevailing atmospheric wind systems and hence air-sea heat exchange. These dynamic processes provide an efficient mechanism to amplify small changes in insolation into relatively large changes in OHC. Over long time periods the ocean's interior acts like a capacitor and builds up large (positive and negative) heat anomalies that can mitigate or amplify small radiative perturbations as seen in the Holocene trend and Common Era anomalies, respectively. Evidently the ocean's interior is more sensitive to small external forcings than the global surface ocean because of the high sensitivity of heat exchange in the high-latitudes to climate variations.



## 1. Introduction

The debate about the apparent slow down in the rate of global surface warming during the 1999–2013 decade despite the unabated rise in greenhouse gas (GHG) emissions has brought more attention to the role of the ocean in climate change both among scientists and the general public. The ocean constitutes the largest heat reservoir in the Earth's energy budget due to the high heat capacity of water and large volume and thus plays an important role in mediating the Earth's climate (Levitus et al., 2012). Ongoing research suggests that an increased rate of heat uptake by the ocean's interior may have negated some of the surface warming arguably leading to the apparent slow down in the rate of global warming (e.g., Balmaseda et al., 2013; Levitus et al., 2012; Meehl et al., 2013; Trenberth and Fasullo, 2013), (Fig. 1). Modern estimates of the change in ocean heat content (OHC) go back only to 1955, however the accuracy of the early data sets is debated (https://www.nodc.noaa.gov/OC5/3M_HEAT_CONTENT/). Since 2006 more accurate estimates have become available from the ARGO array, and they are generally consistent with estimates from the early observations suggesting a relatively constant rate of OHC increase since the early 1990s (Roemmich et al., 2015). A recent compilation suggests that since 1955, ~90% of the excess heat went into the ocean raising concerns about the future state of the oceans (Laffoley and Baxter, 2016). However, given the small magnitude, the brevity of the observed changes in deep OHC and uncertainties of the spatial extent of the current anomalies, any future projection

* Corresponding author.
*E-mail addresses:* rosentha@marine.rutgers.edu (Y. Rosenthal), jkalansky@ucsd.edu (J. Kalansky), audrey.morley@nuigalway.ie (A. Morley), linsley@ldeo.columbia.edu (B. Linsley).

http://dx.doi.org/10.1016/j.quascirev.2016.10.017

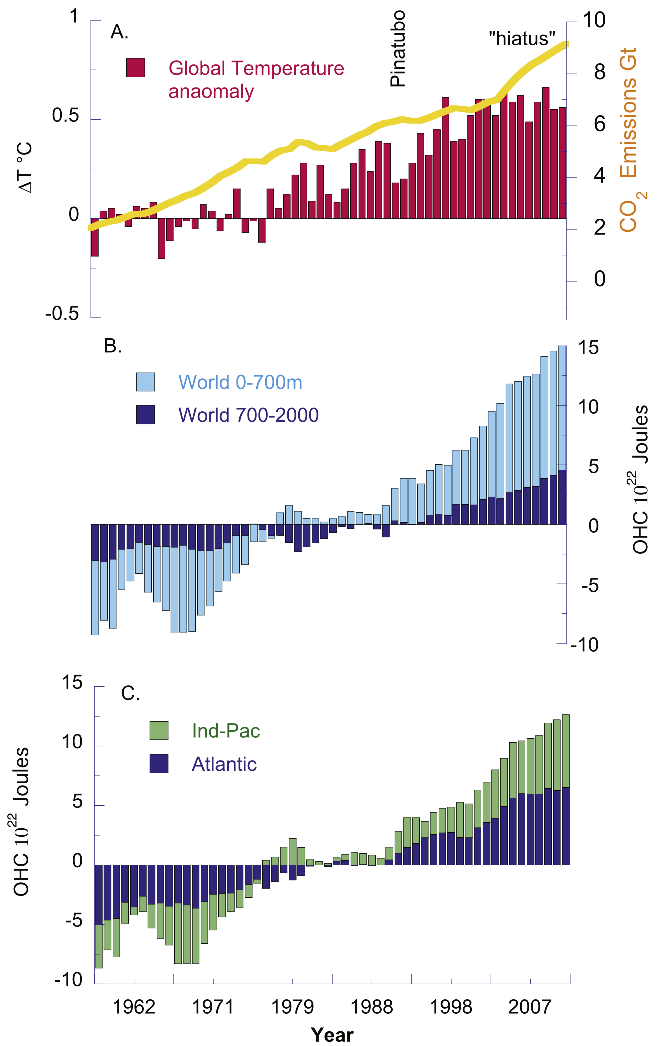


**Fig. 1.** The last 60 years carbon emissions are shown (A) global surface temperature anomalies are compared with global emissions of $CO_2$; (B) changes in World Ocean OHC at different depth intervals; (C) changes in OHC at different ocean basins.

depends on our understanding of the mechanisms controlling changes in the ocean's interior heat content.

While ocean heat uptake is directly related to the radiative forcing and climate sensitivity (e.g., Hansen et al., 1984), the rate of heat uptake/release by the ocean is dependent, to a large extent, on dynamic processes controlling air-sea exchange at key locations. The exact nature of these processes is, however, debated. For example, it is still unclear if the largest contribution to the current increase in OHC is due to dynamic changes in the equatorial or the higher latitude oceans.

There is mounting evidence that multiple mechanisms are driving the Pacific Decadal Oscillation (PDO) and that some of these processes are also sensitive and/or related to Pacific OHC (e.g., Balmaseda et al., 2013; England et al., 2014; Meehl et al., 2013; Newman et al., 2016; Thompson et al., 2015; Trenberth and Fasullo, 2013). While the mechanisms controlling the variability of the PDO are still investigated, their global-scale importance is now recognized with the realization that decadal-scale anomalies in surface temperatures, trade winds, sea level pressure and rainfall in the Pacific basin that have developed since the start of the recent hiatus in Earth surface warming (~1999) resemble the negative phase of the PDO (Trenberth and Fasullo, 2013). During this current negative phase of the PDO, the North and South Pacific central gyres and western equatorial Pacific are warmer than average, while the eastern equatorial Pacific is cooler than average (Balmaseda et al., 2013; Meehl et al., 2013; Trenberth and Fasullo, 2013; Trenberth et al., 2014). Recent modeling efforts in conjunction with analysis of ARGO float data indicate elevated heat storage in the Pacific water column during this most recent negative phase of the PDO (Balmaseda et al., 2013; England et al., 2014; Kosaka and Xie, 2013; Meehl et al., 2013; Roemmich et al., 2015; Trenberth and Fasullo, 2013) supporting the arguments that the tropical and mid-latitude regions of the Pacific Ocean are important sites of heat exchange between the ocean and the atmosphere. In the subtropics of the Pacific and Atlantic, surface waters can seasonally descend away from the surface along isopycnal surfaces to sub-thermocline depths and flow towards the equator. This process is referred to as the shallow meridional overturning cell. An unprecedented strengthening of the Pacific Ocean shallow overturning cells related to trade wind strengthening has been suggested as the primary cause of the enhanced oceanic heat gain via this subtropical route (Balmaseda et al., 2013; England et al., 2014; Trenberth and Fasullo, 2013). Stronger trade winds coupled with changes in ocean circulation associated with the PDO phase switch in 1999–2000 have resulted in a cooling of the equatorial surface ocean over the last 15 years (England et al., 2014; Trenberth and Fasullo, 2013).

Equatorial processes mainly affect the heat content of the thermocline and may also affect the upper water column (0–700 m). However, a significant amount of warming (~30%) is observed at intermediate ocean depths (Balmaseda et al., 2013; Roemmich et al., 2015). This warming has arguably been attributed to high latitude processes both in the North Atlantic and the Southern Ocean. Based on the reanalysis of hydrographic data collected since 1970 it has been argued that a large part of the recent increase in OHC, particularly below 1000 m, occurred in the Atlantic. Accordingly, the heat gain may be due to the enhancement of the Atlantic Meriodional Overtruning Circulation (AMOC) in response to the recurrent salinity anomaly in the subpolar North Atlantic (Balmaseda et al., 2013; Chen and Tung, 2014). Accordingly, the recovery from the great salinity anomaly of the mid 20th century (Curry et al., 2003), led to the increase in surface density, which would have enhanced vertical convection in the Labrador Sea and subpolar region leading to greater sequestration of heat and $CO_2$. This observation-based hypothesis is consistent with model results suggesting that variations in the strength and depth of the AMOC plays a key role in transporting and redistributing thermal energy to depth, thus regulating the heat capacity of the ocean in response to climate change (Kostov et al., 2014).

An alternative, though not a mutually exclusive explanation, attributes the global increase in OHC at intermediate depths (~700–1400 m) to greater heat gain from surface ocean-atmospheric interactions in the Southern Ocean (Roemmich et al., 2007, 2015). The greater heat gain in the Southern Ocean could be partly caused by the faster warming rate of the Southern vs. Northern Hemisphere high latitudes and the greater area of the Southern Ocean. However, it has been proposed that the strengthening of the Southern Westerly Winds (SWW) and resultant spin up of the subtropical gyres, played a more important role in enhancing the heat gain in the southern high latitudes. The strengthening and poleward shift of the SWW occurred in response to a positive Southern Annular Mode since ~1970 (Thompson et al., 2011). The poleward shift of the SWW enhances the large-scale upwelling in the Southern Ocean due to Ekman divergence south of the Polar Front (~50°S), thus bringing deep colder water to the surface, which in turn promotes heat and gas uptake from the atmosphere. Continuous upwelling and relatively quick northward transport of the cold waters at the surface limits the surface warming in this region thereby sustaining efficient heat uptake (Morrison et al., 2016; Russell et al., 2006). For example, in model simulations a poleward intensification of the SWW results in substantially higher heat and $CO_2$ uptake in the Southern Ocean compared with a model run with a more equatorward position of the SWW, suggesting that air-sea heat exchange in the Southern Ocean may be dominated by dynamic processes (e.g., Russell et al., 2006; Stouffer et al., 2006).

The brevity of the observational record makes it difficult to understand the relative importance of the mechanisms controlling changes in OHC and the role of the ocean in climate. This is because the properties of the deep, and to a lesser extent, intermediate water masses reflect climate perturbations at the surface, which are integrated over relatively long time scales due to the long residence time of these water masses and their tendency to reach a steady state through mixing and diffusion. A longer perspective on changes in OHC, obtained from paleoceanographic proxy records helps to understand the role of the different processes in climate change over various time scales (decades to millennia) and provides a baseline to evaluate the current instrumental observations. Here we review currently available records of Mg/Ca-derived sea surface and intermediate water temperatures (SST and IWT, respectively) through the Holocene, Common Era and some equatorial Pacific coral records covering the recent decades, periods characterized by very different external forcings. The records show substantial changes in intermediate ocean temperature and inferred OHC during these time intervals. Because the changes in mean annual radiative forcing were minimal, we hypothesize that changes in oceanic and atmospheric dynamics, in response to small changes in radiative forcings, were the main control on ocean heat exchange and OHC during the Holocene and Common Era.

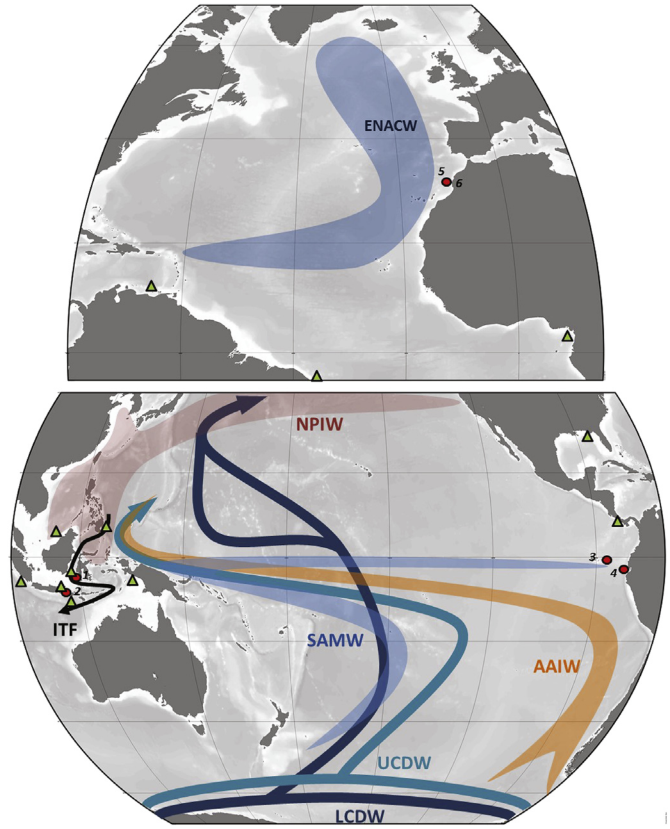


**Fig. 2.** Map of sites used for reconstructing surface and intermediate water temperatures. Also shown are the general trajectories of the modern intermediate water masses (LCDW = Lower Circumpolar Deep Water, UCDW = Upper Circumpolar Deep Water; SAMW = Subantarctic Mode Water; AAIW = Antarctic Intermediate Water; NPIW = North Pacific Intermediate Water; ITF = Indonesian Throughflow). SST records (shown in green triangles) are from Marcott et al. (2013). IWT records (shown in numbered circles) are from Rosenthal et al. (2013) (1&2), Kalansky et al. (2015) (3&4) Morley et al. (2014) (5), and Morley et al. (2011) (6).

## 2. Holocene trends in sea surface temperatures

Insights into the change of OHC can be gained from comparing surface and intermediate-water temperature records reconstructed from foraminifera in sediment cores. Marcot et al. (2013) present a global SST reconstruction for the Holocene based on all the available proxy records at that time. The SST reconstruction shows the Holocene Thermal Maximum (HTM) occurred during the early-to-mid Holocene (10,000–5000 years ago) followed by a ~0.7 °C cooling toward the Little Ice Age (LIA). The HTM timing differs among sites but generally suggests ~0.5° warmer temperatures than recorded at the core tops. The interpretation of this cooling trend as reflecting mean annual global SST is, however, complicated by the apparently contradicting trends recorded by alkenone and Mg/Ca based records particularly in the tropics (Leduc et al., 2010). While the cause of these offsets is investigated (e.g., Timmermann et al., 2014), here we present a subset of the Marcott et al. (2013) data, based only on SST records derived from Mg/Ca measurements in the mixed-layer foraminifer *Globogerinoides ruber* (s.s) (Fig. 2). This should minimize biases due to ecological and seasonal preferences of the different proxy carriers (e.g., foraminiferal based Mg/Ca and haptophytes derived alkenones). We note, however, that the results from this subset of records are consistent with the combined multi-proxy record of Marcott et al. (2013). We present data from low-latitude sites, compiled into three regions representing the western Pacific warm pool (WPWP) (average of 8 sites), eastern Pacific (average of 3 sites) and the equatorial Atlantic (average of 5 sites). All sites are far from the influence of the polar ice sheets and oceanographic frontal regions and thus should be more representative of the direct climate response to the Holocene radiative perturbations. For consistency, we are using the same age models and temperatures reported in Marcott et al. (2013).

The Mg/Ca reconstructions from all three regions suggest that SSTs during the HTM were warmer by a few tenths of a degree relative to the late Holocene (Fig. 3a–c). Considering the variability among the records, it can be concluded that in the low latitude regions, the HTM and subsequent cooling trend toward the late Holocene were very small (<0.5 °C) consistent with the larger, multi-proxy, compilation (Marcott et al., 2013). There are, however, small differences among regions. The WPWP shows about 0.5 °C cooling trend from the early to late Holocene consistent with earlier studies (Linsley et al., 2010; Stott et al., 2004). The observed SST cooling in the WPWP is apparently at odds with the expected warming from the increase in atmospheric $pCO_2$ through the Holocene and the change in local insolation (Liu et al., 2003; Liu et al., 2014). The apparent discrepancy has been attributed to the possibility that foraminiferal Mg/Ca may be recording seasonal rather than mean annual temperatures (Timmermann et al., 2014). We note, however, that records from both sides of the equator, experiencing opposing insolation trends through the Holocene, show similar trends (Linsley et al., 2010), which seems to suggest that seasonality may not exert the dominant control on the Mg/Ca-based SST records in this region. In the eastern Pacific, reconstructed SST is relatively stable until about 4 ka followed by a ~0.5 °C cooling in the late Holocene. A similar trend is observed in the equatorial Atlantic, with relatively stable SST from 12 to 5 ka followed by a ~0.5 °C cooling from ~4 ka to the present. The late Holocene cooling in the eastern equatorial Pacific, is likely due to the intensification of, coastal upwelling in response to changing

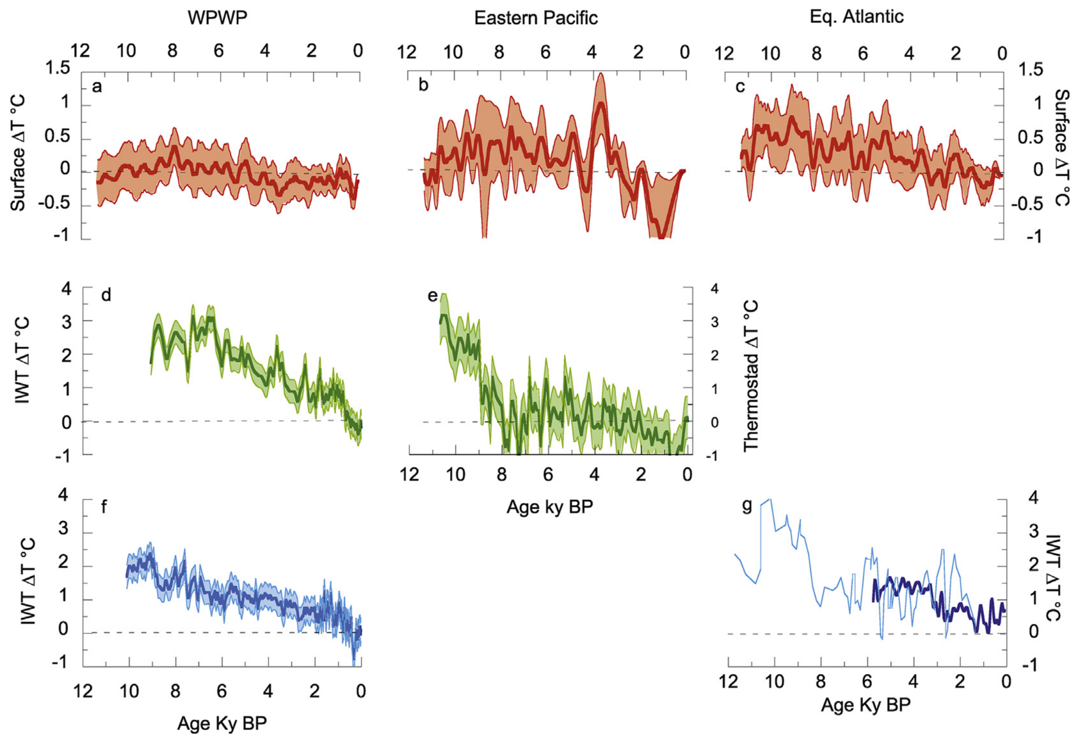


**Fig. 3.** Records of Holocene Mg/Ca-derived SST anomalies (a–c) are compared with IWT anomalies (d–g) from the WPWP, eastern Pacific and North Atlantic.

atmospheric circulation after 4 ka (Nürnberg et al., 2015), which probably also explains the similar trend in paleo-records from the equatorial Atlantic.

## 3. Holocene changes in Pacific OHC

Reconstructing temperature changes of the ocean interior during the Holocene is more challenging due to the limited number of cores with sufficient resolution at intermediate depths. To date, Mg/Ca in benthic foraminifera is the only available proxy for reconstructing deep sea temperatures (see review by Katz et al., 2010). The low temperature sensitivity of Mg/Ca in benthic foraminifera species, typically used for reconstructing Cenozoic and glacial-interglacial changes (e.g., *Planulina wuellerstorfii, Oridorsalis umbonatus and Uvigerina* sp.), and other non-temperature related effects (e.g., the effect of carbonate saturation), often limit their application for reconstructing small changes in intermediate water temperatures. However, a recent calibration of *Hyalinea balthica*, a shallow infaunal species abundant in neritic to upper bathyal and shelf sediments, offers a more sensitive paleothermometer suitable for reconstructing IWT. Core top calibrations suggest a temperature sensitivity of ~12% per °C, which is about four times higher than observed in deep sea benthic foraminifera (Rosenthal et al., 2011). The challenge is, however, to find sites that intersect the major oceanic water masses, have high accumulation rates and contain this foraminifera species.

Over the past several years we have generated several intermediate depth records from three key locations in the western and eastern equatorial Pacific (Fig. 3d–f) and northeastern subtropical Atlantic (Fig. 3g). We discuss additional IWT reconstructions from the North Atlantic and North Pacific, however these are, based on Mg/Ca records from the benthic species *Hoeglunandina elegans* (Came et al., 2007) and *C. wuellerstorfi* (Kubota et al., 2015), which have much lower temperature sensitivity relative to *H. balthica* and thus should be treated cautiously. The intermediate water records at all three regions suggest 2 ± 0.5 °C warmer temperatures during the early Holocene relative to the pre-industrial late Holocene. The pattern of the HTM and subsequent cooling of IWT toward the modern is different than, and exceeds the magnitude seen at the overlying surface. These differences suggest that the long-term Holocene trends in IWT are not directly driven by changes in local radiative forcing but more likely are sourced from the high latitude and transported as heat anomalies to the ocean's interior.

A closer examination of the changes in each region helps to understand the sources and mechanisms behind the reconstructed changes. The western equatorial Pacific records are based on Mg/Ca measurements of the benthic foraminifera *H. balthica* from four cores constituting a bathymetric transect (~500–900 m water depth) in the Makassar Strait and Flores Sea in Indonesia (Rosenthal et al., 2013). This region is well suited to reconstruct mean western Pacific OHC, as thermocline and intermediate water masses found there form in the mid- and high-latitudes of both the northern and southern Pacific Ocean. These water masses can be traced by their distinctive salinity and density as they flow towards the equator (Fine et al., 1994; Gordon, 2005; Rosenthal et al., 2013). Here, the modern thermocline (~200–500 m) is dominated by North Pacific Intermediate Water (NPIW) contributing to the Indonesian Throughflow (ITF), which flows into the Indian Ocean. The relatively uniform water mass below the main thermocline (~450–1000 m) known as Indonesian Intermediate Water forms in the Banda Sea via strong vertical mixing between shallow/warm/relatively fresh and deep/cold/relatively salty waters (Gordon, 2005; Talley and Sprintall, 2005). At intermediate depths, the northwestward flowing New Guinea Coastal Undercurrent, which originates in the South Pacific, flows through the Indonesian passages and reaches the Banda Sea, carrying a significant contribution of Antarctic Intermediate Water (AAIW) (Zenk et al., 2005). The IWT records from the Makassar Strait show cooling trends from the early-mid to the late Holocene of about 2.2 ± 0.4 at 500 m and 1.5 ± 0.3 °C at 600–900 m (Rosenthal et al., 2013). Based on the modern hydrography and given the similarity of the records at all depths, we have argued that Holocene IWT changes in the western equatorial Pacific are linked to climate variability in both the northern and southern high latitudes (Rosenthal et al., 2013). However, because of the vigorous deep mixing in the Banda Sea, a link to either of the hemispheres could not unequivocally be established.

Water at the base of the eastern equatorial Pacific (EEP) thermocline, known as the thermostad (~150–350 m water depth) or 13 °C Mode Water (Tsuchiya, 1981) is linked to the Southern Ocean through the influence of Subantarctic Mode Water (SAMW) (Kalansky et al., 2015); and references therein). A Mg/Ca record of deep dwelling planktonic foraminifer (*Neogloboquadrina dutertrei* with an estimated depth habitat of ~120 m below surface in the EEP region) from a core situated at 375 m water depth on the Peru Margin suggests higher temperatures during the early Holocene and a sharp cooling of ~2° by ~8 ka (Kalansky et al., 2015). After a relatively stable period between ~7 and 4 ka, there is an additional ~1 °C cooling to the present (Fig. 3e). The strong covariance with the bottom temperature reconstruction from the benthic foraminifer *Uvigerina* spp. in this core suggests that the planktonic record primarily represents changes in thermocline temperature/depth likely linked to climate change in the Southern Ocean (Kalansky et al., 2015). Antarctic ice cores (Masson-Delmotte et al., 2011; Mulvaney et al., 2012), terrestrial records (Verleyen et al., 2011) and Southern Ocean temperature reconstructions (Shevenell et al., 2011) show warming associated with the Younger Dryas and a near synchronous early HTM (~11.5–9 Ka) followed by a sharp cooling by ~8 ka. Based on the similarity with these records, it has been argued that the early Holocene temperature change in the thermostad originated in the southern high latitudes and was advected to the EEP thermostad by SAMW (Kalansky et al., 2015). Foraminiferal $\delta^{13}C$ and εNd records from the eastern equatorial Pacific support the greater influence of Southern Ocean water on the thermostad during the late deglaciation and early Holocene (Pena et al., 2008, 2013; Spero and Lea, 2002).

Elevated thermostad temperatures during the early Holocene have been linked to regional changes in climate conditions in the Southern Ocean (Kalansky et al., 2015). Particularly a more southward position of the SWW during the early Holocene enhanced the contribution of warm subtropical water to the forming SAMW and the eastern equatorial Pacific thermostad (Bostock et al., 2013; Bova et al., 2015). Based on opal accumulation records from cores in the South Atlantic and SW Pacific it has been argued that the SWW shifted southward after the Antarctic Cold Reversal (~13 Ka; Anderson et al., 2009), and likely remained in a more poleward position until around 9–8 ka. This hypothesis is supported by different lines of paleoceanographic evidence including temperature records from Antarctic ice cores (e.g., Masson-Delmotte et al., 2011; Mulvaney et al., 2012), reconstructions of Antarctic and Subantarctic SST (Bianchi and Gersonde, 2004; Kaiser et al., 2005; Pahnke and Sachs, 2006; Pahnke and Zahn, 2005; Shevenell et al., 2011) and sedimentary evidence for shifts in the precipitations belt in southern America (Bender et al., 2013; Lamy et al., 2010) (Fig. 4).

Models show that AAIW production is strongly related to the location and strength of the SWW. Thus the effect of the SWW is not limited to the Subtropical Front (e.g., Russell et al., 2006; Stouffer et al., 2006). A poleward shift of the SWW and associated polar front during the deglaciation and early Holocene likely led to increased upwelling of relatively warm upper circum polar deep water (UCDW) around Antarctica (Peck et al., 2015; Toggweiler et al., 2006). While flowing northward, the upwelled UCDW was further warmed by heat exchange with the atmosphere before mixing into the newly formed AAIW and SAMW, which contributed

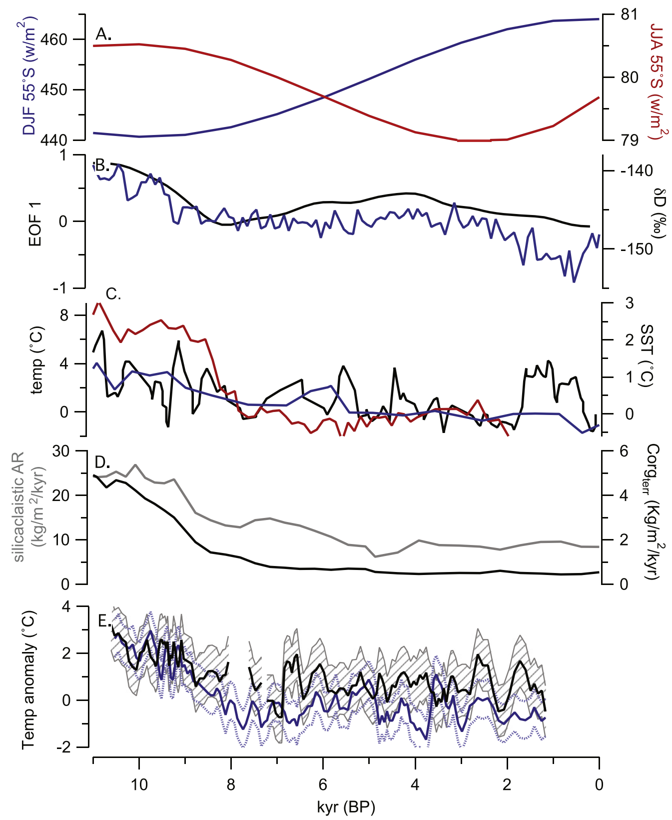


**Fig. 4.** Southern Hemisphere high latitude temperature and precipitation records plotted along with *Uvigerina* and *N. dutertrei* temperature anomalies from the EEP. (A) Dec–Feb and June–August insolation at 55°S latitude (B) Antarctic temperature records from and Empirical Orthogonal Function (EOF) of 5 ice core $\delta^{18}O$ records (black line) (Masson-Delmotte et al., 2011) and James Ross ice core δD (blue line) (Mulvaney et al., 2012) (C) Ocean temperature records (0–150 m) from the Pacific sector of the Southern Ocean (black line) (Shevenell et al., 2011), SST from MD97 2021 (45°S, 174°E) (red line) (Pahnke and Sachs, 2006) and SST from ODP 1233 (41°S, 74°W) (blue line) (Kaiser et al., 2005) (D) $C_{org}$ and siliciclastic accumulation rates as proxies for precipitation from the Chilean Fjords (53°S) (Lamy et al., 2010) (E) *N. dutertrei* (blue) and *Uvigerina* (black) temperature reconstructions from the EEP (Kalansky et al., 2015). Note the different temperature scales on the axes.

to the early Holocene OHC maximum. A northward migration of the SWW and associated polar fronts reduced the contributions of both subtropical surface water and upwelled UCDW to SAMW formation regions thereby leading to progressive cooling of the intermediate water masses originating from the Southern Hemisphere. Migrations of the SWW have been attributed to changes in the Hadley circulation in response to a change in the latitudinal temperature gradient (LTG) (Chiang and Friedman, 2012). On orbital time scales the main mechanism that regulates the latitudinal distribution of insolation and thus the LTG is the interplay between the 41 ka obliquity cycle and the 21 ka precession cycle, which varied significantly throughout the Holocene.

The patterns and timing of these changes were, however, not uniform around the Antarctic region with some sectors showing an early HTM and subsequent cooling to almost modern temperatures by 8 Ka, whereas other regions follow a more Northern Hemisphere pattern with gradual cooling starting at ~7 Ka as recorded for example in Taylor Dome, Antarctica (e.g., Masson et al., 2000; Steig et al., 2000) and sediment records (e.g., Anderson et al., 2009; Hodell et al., 2001; Peck et al., 2015; Shevenell et al., 2011). Thus the signals recorded in intermediate water masses were likely affected by climate variability at the different formation sites, which may explain the differences among our records. As we have no records below 350 m from the EEP, we cannot say whether intermediate water masses in this region experienced comparable changes to the EEP thermostad or to those observed at intermediate depths in the Indonesian cores.

At present the dominant water mass within the lower thermocline of the Makassar Strait (~200–500 m) is the low salinity NPIW (Gordon, 2005). Therefore, Rosenthal et al. (2013) suggested that the shallowest records from the Makassar Strait (~500–600 m) might reflect changes in the properties of the NPIW. NPIW currently forms during the winter by brine rejection and sinking of dense shelf water in the Sea of Okhotsk (Talley, 1991). In contrast with the southern hemisphere, the winter/spring insolation minimum occurred during the early Holocene at high northern latitudes, increasing monotonically towards the present. Alkenone derived SST records show higher SST during the early Holocene in several parts of the Okhotsk Sea and NW Pacific followed by a cooling towards the late Holocene (Harada et al., 2014; Max et al., 2014). This trend is interpreted to reflect warmer late summer/autumn temperatures consistent with the higher summer/autumn insolation at that time. The concurrent reduction in sea ice extent in the Okhotsk Sea have led these authors to argue for a reduction of NPIW production during the early Holocene. A low-resolution Mg/Ca record generated from the benthic foraminifer *C. wuellerstorfi* extracted from a core on the continental slope east of Okinawa Island (1166 m water depth) may provide insight on the Holocene history of NPIW. The low-resolution record shows no discernible trend through the Holocene (Kubota et al., 2015) suggesting that the observed changes in the Makassar sites might not be related to changes in the formation of NPIW. A similar interpretation is drawn from a benthic foraminifera record of mid-water depth radiocarbon content in the northwest Pacific Ocean indicating that NPIW ventilation was stronger in the early (~9–6 Ka) than the late Holocene (~2.5–1.5 Ka), apparently in contrast with the interpretations of sea surface conditions in the Okhotsk Sea and northwest Pacific (Max et al., 2014; Rella and Uchida, 2014). The decoupling between the radiocarbon derived changes in NPIW ventilation, and surface conditions in the northern Pacific led the authors to suggest that at intermediate depths, the NW Pacific might have responded to changes in the Southern Ocean overturning forced by latitudinal displacements of the SWW (Rella and Uchida, 2014). Accordingly, enhanced ventilation of NPIW during the early Holocene, observed in a core off Japan, is due to a stronger contribution of AAIW to the NW Pacific and enhanced mixing with the overlying NPIW. If these interpretations are correct, temperature changes observed in our Indonesian cores within the lower thermocline might have also been sourced from the Southern Hemisphere due to wind induced convective processes associated with the Southerly Jet.

## 4. Holocene changes in Atlantic OHC

Recent changes in North Atlantic intermediate and deepwater temperatures are possibly related to variations in the AMOC in response to recent anomalies in the sub polar gyre (SPG) surface salinities (Balmaseda et al., 2013; Chen and Tung, 2014). Temperature reconstruction, based on a Mg/Ca record from the benthic species *Hoeglunandina elegans* from a sediment core on the flanks of the Little Bahama Bank (LBB) at 1057 m water depth suggests that IWT was >2 °C warmer during the early Holocene than today (Fig. 3). The ~1.5 °C cooling after 8 ka. is likely due to the cooling of high latitude North Atlantic surface waters, where this intermediate water mass is formed (Came et al., 2007). A higher resolution *H. balthica* Mg/Ca record from ~900 m water depth in the northeastern subtropical Atlantic shows a further ~1 °C cooling at ~3.5 ka in response to climate variability at the North Atlantic high-latitudes (Morley et al., 2011). The core, situated in the northeastern part of the Atlantic on the African margin, is under the influence of Eastern North Atlantic Central Waters (ENACW), an intermediate water mass that largely consists of Subpolar Mode Water (SPMW) and therefore is highly susceptible to ocean-atmosphere interactions in the region of the SPG. Morley et al. (2011) showed that past temperatures and salinity of ENACW recorded off the Northwest African continental margin are determined by SPMW formation south and west of Iceland on both instrumental, multidecadal and multicentennial timescales throughout the Holocene (Bamberg et al., 2010; Morley et al., 2011, 2014). Essentially, ENACW circulation provides an ‘oceanic tunnel’ (Liu and Alexander, 2007) transmitting subpolar ocean-atmospheric climate anomalies to lower latitudes and the oceans interior. SPMW properties (temperature and salinity) in turn depend on (1) the strength of the northern mid-latitude westerlies during the winter, (2) SPG surface ocean dynamics and (3) the freshwater input of East Greenland Current (EGC) waters into the SPMW formation region.

Over the HTM-to-Late Holocene transition the Mg/Ca based intermediate water temperature record shows a distinct ~1 °C cooling of ENACW between 3.3 and 2.6 ka (Fig. 3g). This shift in ENACW hydrography is attributed to 1) high latitude sea surface cooling and increased winter sea ice extent in the Barents Sea, 2) a southeastward advance of the Sub Arctic Front (SAF) south of the Denmark Strait linked to a stronger influence of the EGC in the Irminger and Iceland Seas; and 3) as a result of (2) cooler and fresher SPMW. These changes have been linked to changes in the latitudinal insolation gradient during the Holocene in response to the Holocene changes in northern hemisphere insolation (Morley et al., 2014). The main mechanism that regulates the latitudinal distribution of insolation is the interplay between the 41 kyr obliquity cycle and the 21 ka precession cycle. Both model analysis and proxy data show that high-latitude peak summer insolation and low-latitude minimum winter insolation resulted in reduced latitudinal temperature gradient due to warming in the Arctic (Davis and Brewer, 2008) and cooling in the tropics during the HTM (Bonfils et al., 2004; Davis and Brewer, 2008). The resultant changes in latitudinal temperature gradient over the mid-to late Holocene transition set in motion a chain of positive climate feedback affecting the air-sea heat exchange processes leading to the observed change in ENACW temperature and heat content (Morley et al., 2014).

Weaker latitudinal insolation gradients during the HTM are also likely to have altered atmospheric circulation regimes, especially over the northern mid-latitudes. Modern observations show that weaker latitudinal temperature and air thickness gradients between the poles and the tropics decrease the speed and elongate the wave amplitude of the polar Jet stream resulting in slower moving circulatory systems. The resultant prolonged weather conditions are now referred to as ‘atmospheric blocking’ (Francis and Vavrus, 2012). Häkkinen et al. (2011) propose that ‘atmospheric blocking’ over the subpolar North Atlantic also fundamentally influences ocean circulation and upper ocean air-sea exchange. This is because a more southeasterly position of the mid-latitude Westerlies (Woollings et al., 2008) and weaker storm intensities during weaker LTG lead to a reduction in heat loss over the subpolar North Atlantic which in turn result in a weaker SPG circulation. A weaker SPG circulation is characterized by a North-South oriented gyre that allows warmer and more saline water of subtropical origins to enter the Nordic Seas through the Rockall Trough further weakening the gyre (Hátún et al., 2005). In summary, we suggest that changes in LTG over the mid-to late Holocene transition set in motion a chain of dynamic feedback processes that resulted in the observed response of the North Atlantic OHC (Morley et al., 2014).

## 5. The Common Era

Superimposed on the Holocene trends is significant multi-centennial variability expressed both at the surface and intermediate depths. Northern hemisphere surface temperature reconstructions for the Common Era show 0.8 ± 0.3 °C cooling from the Medieval Climate Anomaly (MCA, between 950 and 1250 CE) to the LIA (between 1550 and 1850 CE) (Mann et al., 2008). In the past 150 years, the NH surface temperature returned to the MCA levels and is likely as warm or warmer than any other time during the last 1300 years (Mann et al., 2008; Moberg et al., 2005). The SST reconstruction from the WPWP, the largest warm water region on the planet, closely follows the Northern Hemisphere temperature reconstruction (Oppo et al., 2009), demonstrating a strong coherence between climate variability in the WPWP and the Northern Hemisphere high latitudes (Fig. 5a). Reconstructions of IWT from Indonesia, spanning depths of ~500–900 m, share strong similarity with surface temperatures except at the last two centuries. Pacific IWT were 0.9 ± 0.3 °C (1 SEE) colder during the LIA than during the MCA. Within age model errors, the IWT cooling from the MCA to LIA is of the same magnitude as (and possibly lags) the cooling of the overlying surface water and the cooling recorded in the Northern Hemisphere. Lowest temperatures occur during the 17–18th centuries both at the surface and intermediate depths. Subsequently the SST and IWT records diverge. Surface temperatures warmed by ~0.5 ± 0.15 °C for the period of 1850–1950 CE, which is remarkably consistent with the instrumental record for the same period returning to MCA levels. In a sharp contrast, modern IWT in Indonesia are about the same as during the LIA (Fig. 5b). The slow recovery of the IWT is not surprising given that in this equatorial site it takes many decades for the intermediate water masses to reach the western equatorial Pacific from their high-latitude origin (Fine et al., 1994). This large lag between the Indonesian IWT records and the changes recorded at the surface suggest that large parts of the ocean interior are not in equilibrium with the recent climate change. A closer link and relatively rapid response between surface ocean/atmosphere conditions and downstream intermediate water temperatures can be seen in the northeastern Atlantic site, situated closer to the possible source region. The 1200 year long benthic foraminiferal Mg/Ca from the ~900 m deep site off northwest Africa discussed above shows strong centennial scale temperature variability on the order of 0.7 °C superimposed on a gradual cooling of ~1 °C from 950 to 1850 CE.

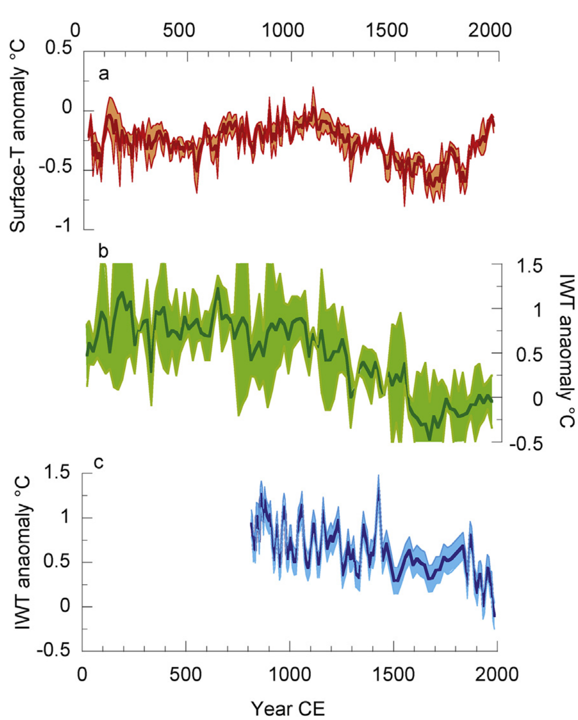


**Fig. 5.** Common Era temperature anomalies. (a) Average surface anomalies based on the reconstructions of Mann et al. (2008), Moberg et al. (2005) and Oppo et al. (2009). (b) IWT anomalies in intermediate water depth (~500–900 m) cores from Indonesia (Rosenthal et al., 2013). (c) IWT anomalies in intermediate water depth (~1000 m) core from the northeastern Atlantic (Morley et al., 2011).

The causes of the last millennium climate anomalies are debated. At present it is thought that the LIA cooling was caused by the combined effects of changes in total solar irradiance (TSI) and explosive volcanic activity (e.g., Crowley (2000). Recent model simulations estimate the direct radiative perturbations during the last millennium to be about $-0.2 \pm 0.1$ W/m$^2$ (e.g., Schmidt et al., 2012) largely due to enhanced explosive volcanism during the LIA and to a lesser extent changes in TSI (Atwood et al., 2016). Models using these forcings, simulate the general climate anomalies of the last millennium as recorded by various proxy reconstructions (Atwood et al., 2016; Landrum et al., 2013). The simulations suggest, however, that the combination of all the direct forcings contribute to only about half of the cooling during the LIA, whereas the rest is driven by positive feedbacks (Atwood et al., 2016).

Simulations of the temperature variability during the last millennium are generally consistent with proxy compilations, suggesting ~0.3 °C global cooling from the MCA to LIA (Atwood et al., 2016; Landrum et al., 2013). Although these anomalies are smaller than suggested from proxy records of surface and subsurface temperatures, the simulations suggest a factor of two or larger anomalies in the polar regions, especially during the cold seasons of intermediate and deep water formation (e.g., Landrum et al., 2013). The implied strengthening in the LTG, and associated expansion of sea ice coverage from the MCA to LIA suggested by the models, could have led to major changes in the atmospheric and oceanographic conditions in the polar regions and are likely the cause of the LIA cooling and decrease in heat content of the eastern North Atlantic central water (Morley et al., 2011). The importance of dynamic processes and feedbacks relative to changes in the background forcing is reflected in the ~0.5 °C cooling of ENACW during the past 150 years. This cooling trend, which seems at first at odds with global warming of ~0.9 °C due to the increase in GHG, is likely related to enhanced sea surface heat loss due to stronger Mid-latitude Westerly Winds over the northeastern SPG since the early 19th century (Morley et al., 2011). This recent cooling trend is also present in SST proxy reconstructions (Hall et al., 2010) and in instrumental SST datasets from the northeastern SPG (Xue et al., 2003) demonstrating the intimate link between surface conditions in the high latitudes and intermediate water OHC in the North Atlantic.

While it is difficult to link changes in IWT recorded in Indonesian cores to their source regions, we assume that similar dynamic mechanisms that were responsible for the Holocene trends also contributed to the last millennium anomalies in intermediate water OHC despite the difference in the forcings. In the Southern Ocean, the enhanced cooling and extended sea ice coverage during the LIA, suggested in model simulations (e.g., Landrum et al., 2013), possibly also resulted in a shift in the SWW. Indeed there are indications of significant cooling during the LIA and possible changes in wind strength and/or position during the LIA (Abram et al., 2013; Chambers et al., 2014; Orsi et al., 2012; Rhodes et al., 2012). These processes could have led to a negative heat anomaly in the formation sites of Antarctic intermediate and mode waters, which could have affected the intermediate water temperatures in the western equatorial Pacific (Rosenthal et al., 2013).

Although the background radiative anomaly throughout the last millennium was very small, significantly larger negative anomalies likely followed major/successive volcanic eruptions resulting in multi decadal length intervals of cooling on the order of 1–1.5 °C (Atwood et al., 2016; Landrum et al., 2013). Models simulating the effects of major volcanic eruptions suggest increased air-sea heat exchange at the southern high latitudes resulting in persistent negative OHC anomalies in subsurface water masses (e.g., Gleckler et al., 2006; Stenchikov et al., 2009). Another simulated consequence of volcanic eruptions is the expansion of sea ice coverage in the Arctic and Nordic Seas that can lead to changes in the AMOC although the exact response differs among models (e.g., Ding et al., 2014; Schleussner and Feulner, 2013). Records of sea ice extent and ice caps growth from Arctic Canada and Iceland (Miller et al., 2012) suggest that the LIA was a result of large explosive volcanism causing cooling and expansion of the sea-ice. This hypothesis is supported by transient modeling suggesting that explosive volcanism can result in Northern Hemisphere summer cooling and expansion of sea-ice, which may persist long after the eruption due to sea-ice/ocean feedbacks, which might contributed to the LIA cooling (Miller et al., 2012). Regardless of the exact mechanism, the models suggest that the negative radiative forcings from an eruption, penetrates to the subsurface within a few years after the eruption but the anomaly persists much longer with slow relaxation persisting for decades and centuries in the mid-depth and deep ocean, respectively (Ding et al., 2014; Stenchikov et al., 2009). We suggest that in addition to the direct negative radiative forcing caused by successive volcanic eruptions (Consortium, 2013), the persistent upwelling of progressively previous negative heat anomalies to the surface contributed to the cooling during the LIA. A similar mechanism has been proposed as a mediating process for the recent global warming (Gleckler et al., 2006; Rosenthal et al., 2013).

## 6. The recent two centuries

Decadal changes in surface conditions in the tropical and subtropical Pacific appear to be another mechanism for regulating upper OHC on decadal time-scales (e.g., England et al., 2014; Meehl et al., 2013; Trenberth and Fasullo, 2013). Linsley et al. (2015) reported evidence of a positive correlation between decadal changes in South Pacific upper OHC and reconstructed subtropical South Pacific SST from a composite of coral core Sr/Ca records from Fiji, Tonga and Rarotonga (FTR). Over the interval of overlap with Levitus et al. (2012) back to 1950, during decades of elevated South Pacific SST, upper ocean heat content in the South Pacific rises. FTR coral Sr/Ca SST and instrumental SST are also inversely correlated with decadal changes in equatorial Pacific coral Sr/Ca SST (see Linsley et al., 2015). In Fig. 6 we compare the FTR composite coral Sr/Ca SST record to 0–700 m upper OHC for the S. Pacific and to an equatorial composite coral $\delta^{18}O$ record generated by averaging results from Fanning Atoll (Cobb et al., 2013), Palmyra (Cobb et al., 2013) and Maiana (Urban et al., 2000) (FPM index, defined in Linsley et al., 2015). Although coral $\delta^{18}O$ can be sensitive to changes in both water temperature and salinity, this comparison suggests that decadal-scale changes in FPM coral $\delta^{18}O$ are in part driven by changes in SST and demonstrates the opposite response of the equatorial and subtropical South Pacific on decadal time-scales. Collectively, these results and those presented in Linsley et al. (2015), in combination with other conclusions drawn from paleo and instrumental data analysis (e.g., England et al., 2014; Thompson et al., 2015), indicate that over the past century, decades of stronger trade winds during negative phases of the PDO resulted in elevated equatorial upwelling rates and generally cooler SST near the equator. Based on data from primarily the late 20th century, England et al. (2014) proposed the link between increased trade winds, cool equatorial SSTs, intensified wind stress curl on either side of the equator and a spin up of the subtropical gyres to explain both the increase in subduction of warm subtropical water into the ventilated thermocline and the increase in subsurface heat uptake in the western equatorial Pacific. The equatorial and South Pacific coral results are completely consistent with this hypothesis. The 206 year long (1997–1791) FTR coral Sr/Ca reconstruction of Linsley et al. (2015) also indicate persistent decadal SST variability back to 1791 with a mean recurrence interval of approximately 25 years. This multi-century coral–based record thus supports the hypothesis that semi-periodic decadal-scale changes in equatorial and subtropical Pacific surface ocean-atmosphere conditions are involved in regulating heat storage in the upper ocean.

## 7. Causes and implications of Holocene OHC change

Ocean temperature reconstructions presented here suggest that the HTM warmth and subsequent cooling of intermediate water masses were not likely restricted only to the western equatorial Pacific as previously documented (Rosenthal et al., 2013). Although, the available record from the North Pacific apparently shows no significant cooling through the Holocene (Kubota et al., 2015), records of intermediate waters from the North Atlantic provide evidence for Holocene cooling, consistent with the records from Indonesia. Likewise, the reconstructed IWT changes from the MCA to the LIA seem to have affected intermediate water masses in both the Pacific and Atlantic Oceans. Both the long-term trend cooling throughout the Holocene and the anomalies during the Common Era i.e., the transition from the warm MCA to the cold LIA provide interesting case-studies of changes in OHC under different natural conditions that can be compared with the anthropogenically-driven changes over the past several decades. This is because the external forcings during each of these periods were very different. The largest external forcing throughout the Holocene was due to precessionally-driven changes in seasonal insolation, which is anti-phased between the hemispheres. However, the apparent coherency among records influenced by water masses originating both in the northern and southern hemisphere suggests that the observed trends in IWT cannot be directly driven by insolation. While obliquity has symmetric effect on both hemispheres the total change in mean annual insolation from the early to late Holocene was $\ll 1$ W/m$^2$ at the latitudes where these intermediate water masses form (45–55°). As discussed above, the interaction between precession and obliquity not only changed local insolation but also latitudinal temperature gradients, which strongly affect the prevailing atmospheric systems and hence air-sea heat exchange. These dynamic processes provide an efficient mechanism to amplify the small changes in orbital forcing, into relative large changes in OHC.

Orbitally-driven changes in insolation were minimal during the last millennium and cannot explain the changes in the Common Era. Instead, the MCA to LIA cooling is attributed to the effects of volcanic eruptions and variations in total incoming insolation (TSI) causing a negative radiative forcing on the order of $-0.2 \pm 0.1$ W/m$^2$. It is generally assumed that the effects of direct forcing through the last millennium were relatively uniform in both hemispheres, much like the effects of the recent increase in GHG though with substantially smaller impact compared with the estimated total anthropogenic radiative forcing of $+1.6 \pm 0.8$ W/m$^2$ (Forster and Ramaswamy, 2007).

Recent model simulations using Flexible-Ocean-Atmosphere-Land model suggests that the changes in insolation during the HTM could have led to significant changes in ocean heat uptake, especially due to the strong warming in the Southern Ocean high

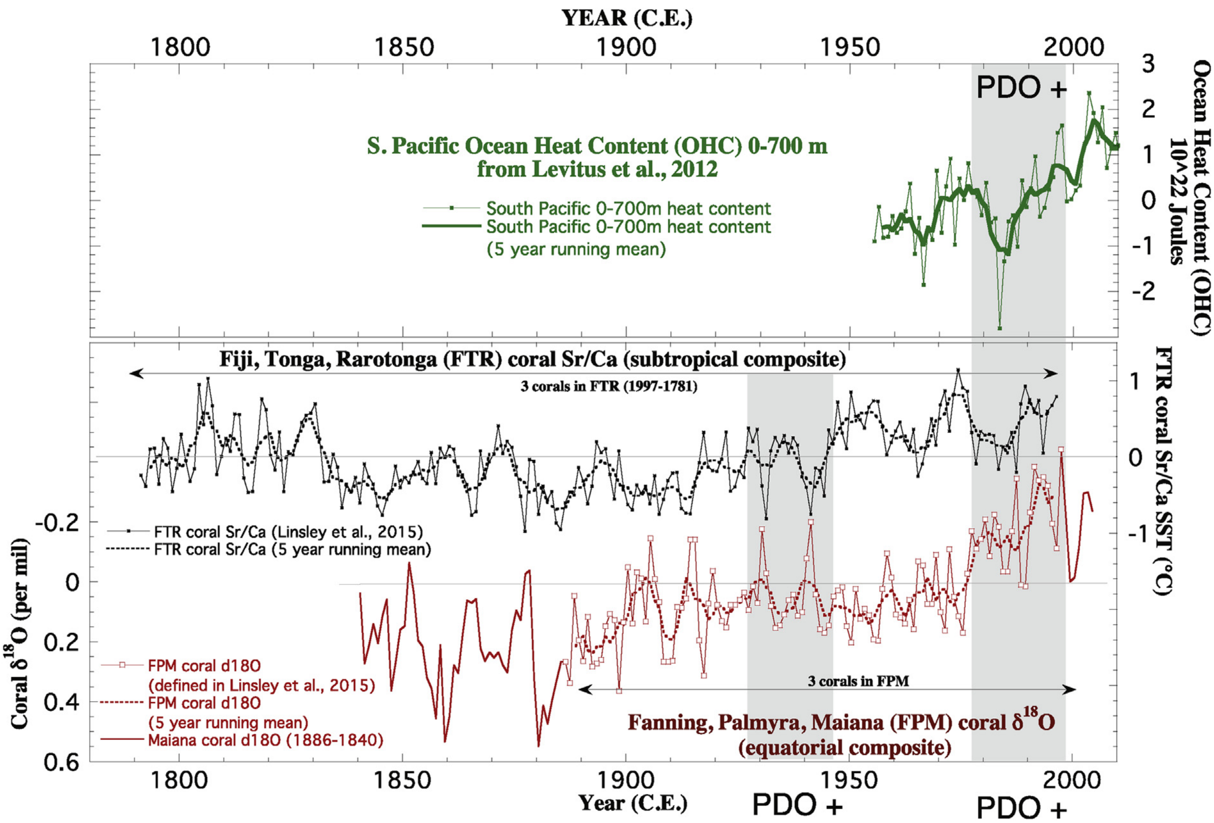


**Fig. 6.** (top) Comparison of South Pacific 0–700 m Ocean Heat Content (in $10^{22}$ J; Levitus et al., 2012) to (middle) Fiji, Tonga, Rarotonga (FTR) coral Sr/Ca SST reconstruction of Linsley et al. (2015) and (bottom) Fanning, Palmyra, Maiana (FPM) equatorial coral $\delta^{18}O$ composite (defined in Linsley et al., 2015). The number of corals comprising each average is indicated. Fanning and Palmyra data from Cobb et al. (2013) and Maiana data from Urban et al. (2000).

latitudes (Luan et al., 2016). Although the magnitude of the simulated warming is significantly smaller than recorded in our cores and it is restricted to depths greater than 1000 m, the results generally support our argument that warming of the intermediate depths in the equatorial Pacific probably originated in the Southern Ocean much as is the case at present. The MCA simulation shows a more uniform warming of the ocean interior at all depths and indicates heat uptake both in the northern and southern hemispheres. It is possible that the difference between the model results and the paleo-data is because the models do not accurately mimic the dynamic, likely wind-driven, processes that exert large control on the ocean-atmosphere heat exchange, especially in the high latitudes. To better quantify these processes we'll need not only to "fine tune" the models but also to increase the distribution of the paleo-records to capture the full depth and geographical extent of the changes. This is important because evidently small differences in the heat exchange rate can lead to very large changes in OHC.

Based on the IWT records from the Indonesian region, Rosenthal et al. (2013) suggested that Pacific OHC was likely much higher during the HTM than in the late Holocene, and during the MCA than the LIA. Although the timing of the HTM and subsequent cooling is not synchronous among sites, likely reflecting variable climate conditions at the different source regions of these water masses, the available records suggest that estimates of OHC provided by Rosenthal et al. (2013) (Fig. 7) are probably conservative. Likewise, the reconstructed IWT changes from the MCA to the LIA likely affected intermediate water masses in both the Pacific and Atlantic Oceans. Levitus et al. (2012) report a mean ocean warming of the 0–700 m ocean layer of 0.18 °C between 1955 and 2010, corresponding to +0.033 °C per decade. To obtain a first order comparison, we assume that our records represent the World Ocean and thus are comparable in volume with the current estimates (Levitus et al., 2012). Assuming the intermediate depth ocean (0–700 m) cooled between 10 and 2 Ka by ~1.5 °C we calculate a cooling rate −0.002 °C per decade. Similarly, considering the intermediate depth ocean (0–700 m) cooled by ~0.5 °C between 1200 and 1600 CE we calculate a temperature change of −0.013 °C per decade. In both cases these rates are smaller than the modern rates even when applying the observed IWT changes to the whole ocean (as opposed to just the Pacific as was done in Rosenthal et al. (2013).

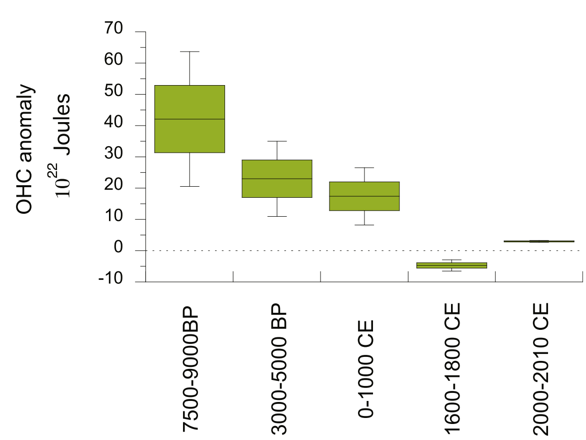


**Fig. 7.** Reconstructed anomalies in Pacific OHC in the 0–700 m depth interval for the early-Holocene, mid-Holocene, MWP and LIA periods. Reconstructed anomalies are calculated relative to the reference period of 1965–1970 CE (Rosenthal et al., 2013).

These crude estimates demonstrate that small but persistent perturbations in the earth energy budget can result in large anomalies in IWT and consequently OHC. To put it differently, a warming rate of +0.004 °C per decade over the last deglaciation (~20–10 Ka) would have caused an ocean warming of ~4 °C. These estimates further underscore the argument made by Rosenthal et al. (2013) that over a long time the ocean's interior acts like a capacitor and builds up large (positive and negative) heat anomalies that can mitigate or amplify global temperature change as seen in the Holocene trend and Common Era anomalies, respectively. Evidently the deep ocean is more sensitive to small external forcings than the global surface ocean because of the high sensitivity of heat exchange in the high-latitudes to climate variations. However, the redistribution of the heat in the ocean interior can affect ocean circulation and consequently air-sea heat exchange. The paleo-record suggests that the nature of this feedback process (positive or negative) may change but model simulations are required to explore this. It is therefore important to realize that much as was the case for ocean acidification, warming of the ocean interior may have unappreciated consequences for future climate and marine life (Laffoley and Baxter, 2016).

## Acknowledgements

We would like to acknowledge Paula Moffa-Sanchez for commenting on the manuscript. Y.R. thanks Isabel Hong for help with Adobe Illustrator. Research discussed in this review article was supported by NSF funding (OCE1045377&1003400).

## References

Abram, N.J., Mulvaney, R., Wolff, E.W., Triest, J., Kipfstuhl, S., Trusel, L.D., Vimeux, F., Fleet, L., Arrowsmith, C., 2013. Acceleration of snow melt in an Antarctic Peninsula ice core during the twentieth century. Nat. Geosci. 6, 404–411.
Anderson, R.F., Ali, S., Bradtmiller, L.I., Nielsen, S.H.H., Fleisher, M.Q., Anderson, B.E., Burckle, L.H., 2009. Wind-driven upwelling in the Southern Ocean and the deglacial rise in atmospheric CO2. Science 323, 1443–1448.
Atwood, A.R., Wu, E., Frierson, D.M.W., Battisti, D.S., Sachs, J.P., 2016. Quantifying climate forcings and feedbacks over the last millennium in the CMIP5–PMIP3 models. J. Clim. 29, 1161–1178.
Balmaseda, M.A., Trenberth, K.E., Källén, E., 2013. Distinctive climate signals in reanalysis of global ocean heat content. Geophys. Res. Lett. 40, 1754–1759.
Bamberg, A., Rosenthal, Y., Paul, A., Heslop, D., Mulitza, S., Rühlemann, C., Schulz, M., 2010. Reduced North Atlantic central water formation in response to Holocene ice sheet melting. Geophys. Res. Lett. 37, L17705, 17710.11029/12010GL043878.
Bender, V.B., Hanebuth, T.J.J., Chiessi, C.M., 2013. Holocene shifts of the Subtropical Shelf Front off southeastern South America controlled by high and low latitude atmospheric forcings. Paleoceanography 28, 481–490.
Bianchi, C., Gersonde, R., 2004. Climate evolution at the last deglaciation: the role of the Southern Ocean. Earth Planet. Sci. Lett. 228, 407–424.
Bonfils, C., de Noblet-Ducoudré, N., Guiot, J., Bartlein, P., 2004. Some mechanisms of mid-Holocene climate change in Europe, inferred from comparing PMIP models to data. Clim. Dyn. 23, 79–98.
Bostock, H.C., Barrows, T.T., Carter, L., Chase, Z., Cortese, G., Dunbar, G.B., Ellwood, M., Hayward, B., Howard, W., Neil, H.L., Noble, T.L., Mackintosh, A., Moss, P.T., Moy, A.D., White, D., Williams, M.J.M., Armand, L.K., 2013. A review of the Australian–New Zealand sector of the Southern Ocean over the last 30 ka (Aus-INTIMATE project). Quat. Sci. Rev. 74, 35–57.
Bova, S.C., Herbert, T., Rosenthal, Y., Kalansky, J., Altabet, M., Chazen, C., Mojarro, A., Zech, J., 2015. Links between eastern equatorial Pacific stratification and atmospheric CO2 rise during the last deglaciation. Paleoceanography 30, 1407–1424.
Came, R.E., Curry, W.B., Oppo, D.W., Broccoli, A.J., Stouffer, R.J., Lynch-Stieglitz, J., 2007. North Atlantic Intermediate Depth Variability during the Younger Dryas: Evidence from Benthic Foraminiferal Mg/Ca and the GFDL R30 Coupled Climate Model. In: Geophysical Monograph Series, vol. 173. American Geophys. Union.
Chambers, F.M., Brain, S.A., Mauquoy, D., McCarroll, J., Daley, T., 2014. The 'Little Ice Age' in the Southern Hemisphere in the context of the last 3000 years: peat-based proxy-climate data from Tierra del Fuego. Holocene 1–8. http://dx.doi.org/10.1177/0959683614551232.
Chen, X., Tung, K.-K., 2014. Varying planetary heat sink led to global-warming slowdown and acceleration. Science 345, 897–903.
Chiang, J.C.H., Friedman, A.R., 2012. Extratropical cooling, interhemispheric thermal gradients, and tropical climate change. Annu. Rev. Earth Planet. Sci. 40, 383–412.
Cobb, K.M., Westphal, N., Sayani, H.R., Watson, J.T., Di Lorenzo, E., Cheng, H., Edwards, R.L., Charles, C.D., 2013. Highly variable el niño–southern oscillation throughout the Holocene. Science 339, 67–70.
Consortium, P.k., 2013. Continental-scale temperature variability during the past two millennia. Nat. Geosci. 6, 339–346.
Crowley, T.J., 2000. Causes of climate change over the past 1000 years. Science 289, 270–277.
Curry, R., Dickson, B., Yashayaev, I., 2003. A change in the freshwater balance of the Atlantic Ocean over the past four decades. Nature 426, 826–829.
Davis, B.A.S., Brewer, S., 2008. Orbital forcing and role of the latitudinal insolation/temperature gradient. Clim. Dyn. 32, 143–165.
Ding, Y., Carton, J.A., Chepurin, G.A., Stenchikov, G., Robock, A., Sentman, L.T., Krasting, J.P., 2014. Ocean response to volcanic eruptions in coupled model intercomparison project 5 simulations. J. Geophys. Res. Oceans 119, 5622–5637.
England, M.H., McGregor, S., Spence, P., Meehl, G.A., Timmermann, A., Cai, W., Gupta, A.S., McPhaden, M.J., Purich, A., Santoso, A., 2014. Recent intensification of wind-driven circulation in the Pacific and the ongoing warming hiatus. Nat. Clim. Change 4, 222–227.
Fine, R.A., Lukas, R., Bingham, F.M., et al., 1994. The western equatorial Pacific: a water mass crossroads. J. Geophys. Res. 99, 25063–25080.
Forster, P., Ramaswamy, V., 2007. Changes in atmospheric constituents and in radiative forcing. IPCC Fourth Assessment Report (AR4). In: Solomon, S., Qin, D., Manning, M., Chen, Z., Marquis, M., Averyt, K.B., Tignor, M., Miller, H.L. (Eds.), Climate Change 2007: the Physical Science Basis. Cambridge University Press, Cambridge, United Kingdom and New York, NY, USA, p. 996 pp.
Francis, J.A., Vavrus, S.J., 2012. Evidence linking Arctic amplification to extreme weather in mid-latitudes. Geophys. Res. Lett. 39.
Gleckler, P.J., Wigley, T.M.L., Santer, B.D., Gregory, J.M., AchutaRao, K., Taylor, K.E., 2006. Volcanoes and climate: krakatoa's signature persists in the ocean. Nature 439, 675–675.
Gordon, A., 2005. Oceanography of the indonesian seas and their throughfow. Oceanography 18.
Häkkinen, S., Rhines, P.B., Worthen, D.L., 2011. Atmospheric blocking and atlantic multidecadal ocean variability. Science 334, 655–659.
Hall, I.R., Boessenkool, K.P., Barker, S., McCave, I.N., Elderfield, H., 2010. Surface and deep ocean coupling in the subpolar North Atlantic during the last 230 years. Paleoceanography 25.
Hansen, J., Lacis, A., Russel, G., Stone, T.P., Fung, I., Rued, R., Levrer, J., 1984. Climate Sensitivity: analysis of feedback mechanisms. In: Takahashi, J.H.a.T. (Ed.), Climate Processes and Climate Sensitivity, Am. Geophys. Union. Mon., pp. 130–163.
Harada, N., Katsuki, K., Nakagawa, M., Matsumoto, A., Seki, O., Addison, J.A., Finney, B.P., Sato, M., 2014. Holocene sea surface temperature and sea ice extent in the Okhotsk and Bering Seas. Prog. Oceanogr. 126, 242–253.
Hátún, H., Sandø, A.B., Drange, H., Hansen, B., Valdimarsson, H., 2005. Influence of the atlantic subpolar gyre on the thermohaline circulation. Science 309, 1841–1844.
Hodell, D.A., Kanfoush, S.L., Shemesh, A., Crosta, X., Charles, C.D., Guilderson, T.P., 2001. Abrupt cooling of antarctic surface waters and sea ice expansion in the south atlantic sector of the Southern Ocean at 5000 cal yr B.P. Quat. Res. 56, 191–198.
Kaiser, J., Lamy, F., Hebbeln, D., 2005. A 70-kyr sea surface temperature record off southern Chile (Ocean Drilling Program Site 1233). Paleoceanography 20 n/a-n/a.
Kalansky, J., Rosenthal, Y., Herbert, T., Bova, S., Altabet, M., 2015. Southern Ocean contributions to the eastern equatorial pacific heat content during the Holocene. Earth Planet. Sci. Lett. 424, 158–167.
Katz, M.E., Cramer, B.S., Franzese, A., Hönisch, B., Miller, K.G., Rosenthal, Y., Wright, J.D., 2010. Traditional and emerging geochemical proxies in foraminifera. J. Foraminifer. Res. 40, 165–192.
Kosaka, Y., Xie, S.-P., 2013. Recent global-warming hiatus tied to equatorial Pacific surface cooling. Nature 501, 403–407.
Kostov, Y., Armour, K.C., Marshall, J., 2014. Impact of the Atlantic meridional overturning circulation on ocean heat storage and transient climate change. Geophys. Res. Lett. 41, 2108–2116.
Kubota, Y., Kimoto, K., Itaki, T., Yokoyama, Y., Miyairi, Y., Matsuzaki, H., 2015. Bottom water variability in the subtropical northwestern Pacific from 26 kyr BP to present based on Mg/Ca and stable carbon and oxygen isotopes of benthic foraminifera. Clim. Past 11, 803–824.
Laffoley, D., Baxter, J.M., 2016. Explaining Ocean Warming: Causes, Scale, Effects and Consequences. IUCN, Gland, Switzerland, p. 456.
Lamy, F., Kilian, R., Arz, H.W., Francois, J.-P., Kaiser, J., Prange, M., Steinke, T., 2010. Holocene changes in the position and intensity of the southern westerly wind belt. Nat. Geosci. 3, 695–699.
Landrum, L., Otto-Bliesner, B.L., Wahl, E.R., Conley, A., Lawrence, P.J., Rosenbloom, N., Teng, H., 2013. Last millennium climate and its variability in CCSM4. J. Clim. 26, 1085–1111.
Leduc, L., Schneider, R., Kim, J.-H., Lohmann, G., 2010. Holocene and Eemian sea surface temperature trends as revealed by alkenone and Mg/Ca paleothermometry. Quat. Sci. Rev. 29, 989–1004.
Levitus, S., Antonov, T.P., Boyer, S., Baranova, O.K., Garcia, H.E., Locarnini, R.A., Mishonov, A.V., Reagan, J.R., Seidov, D., Yarosh, E.S., Zweng, M.M., 2012. World ocean heat content and thermosteric sea level change (0–2000 m), 1955–2010. Geophys. Res. Lett. 39, 5.

Linsley, B.K., Rosenthal, Y., Oppo, D.W., 2010. Evolution of the indonesian Throughflow and western pacific warm pool during the Holocene. Nat. Geosci. 3, 578–583. http://dx.doi.org/10.1038/ngeo1920.
Linsley, B.K., Wu, H.C., Dassié, E.P., Schrag, D.P., 2015. Decadal changes in South Pacific sea surface temperatures and the relationship to the Pacific decadal oscillation and upper ocean heat content. Geophys. Res. Lett. 42, 2358–2366.
Liu, Z., Alexander, M., 2007. Atmospheric bridge, oceanic tunnel, and global climatic teleconnections. Rev. Geophys. 45, 2007.
Liu, Z., Brady, E., Lynch-Stieglitz, J., 2003. Global ocean response to orbital forcing in the Holocene. Paleoceanography 18.
Liu, Z., Zhu, J., Rosenthal, Y., Zhang, X., Otto-Bliesner, B.L., Timmermann, A., Smith, R.S., Lohmann, G., Zheng, W., Elison Timm, O., 2014. The Holocene temperature conundrum. Proc. Natl. Acad. Sci. 111, E3501–E3505.
Luan, Y.-H., Yu, Y.-Q., Zheng, W.-P., 2016. Heat budget analysis in three typical warm periods simulated by FGOALS-s2. Atmos. Ocean. Sci. Lett. 9, 7.
Mann, M.E., Zhang, Z., Hughes, M.K., Bradley, R.S., Miller, S.K., Rutherford, S., Ni, F., 2008. Proxy-based reconstructions of hemispheric and global surface temperature variations over the past two millennia. Proc. Natl. Acad. Sci. 105, 13252–13257.
Marcott, S.A., Shakun, J.D., Clark, P.U., Mix, A.C., 2013. A reconstruction of regional and global temperature for the past 11,300 years. Science 339, 1198–1201.
Masson, V., Vimeux, F., Jouzel, J., et al., 2000. Holocene climate variability in Antarctica based on 11 ice-core isotopic records. Quat. Res. 54, 348–358.
Masson-Delmotte, V., Buiron, D., Ekaykin, A., Frezzotti, M., Gallée, H., Jouzel, J., Krinner, G., Landais, A., Motoyama, H., Oerter, H., Pol, K., Pollard, D., Ritz, C., Schlosser, E., Sime, L.C., Sodemann, H., Stenni, B., Uemura, R., Vimeux, F., 2011. A comparison of the present and last interglacial periods in six Antarctic ice cores. Clim. Past 7, 397–423.
Max, L., Lembke-Jene, L., Riethdorf, J.R., Tiedemann, R., Nürnberg, D., Kühn, H., Mackensen, A., 2014. Pulses of enhanced North Pacific intermediate water ventilation from the Okhotsk sea and bering sea during the last deglaciation. Clim. Past 10, 591–605.
Meehl, G.A., Hu, A., Arblaster, J.M., Fasullo, J., Trenberth, K.E., 2013. Externally forced and internally generated decadal climate variability associated with the interdecadal pacific oscillation. J. Clim. 26, 7298–7310.
Miller, G.H., Geirsdóttir, Á., Zhong, Y., Larsen, D.J., Otto-Bliesner, B.L., Holland, M.M., Bailey, D.A., Refsnider, K.A., Lehman, S.J., Southon, J.R., Anderson, C., Björnsson, H., Thordarson, T., 2012. Abrupt onset of the Little Ice Age triggered by volcanism and sustained by sea-ice/ocean feedbacks. Geophys. Res. Lett. 39.
Moberg, A., Sonechkin, D.M., Holmgren, K., Datsenko, N.M., Karlen, W., 2005. Highly variable Northern Hemisphere temperatures reconstructed from low- and high-resolution proxy data. Nature 433, 613–617.
Morley, A., Rosenthal, Y., deMenocal, P., 2014. Ocean-atmosphere climate shift during the mid-to-late Holocene transition. Earth Planet. Sci. Lett. 388, 18–26.
Morley, A., Schulz, M., Rosenthal, Y., Mulitza, S., Paul, A., Rühlemann, C., 2011. Climate variability and signal propagation via North Atlantic central water formation during the Late Holocene. Earth Planet. Sci. Lett. 308, 161–171.
Morrison, A.K., Griffies, S.M., Winton, M., Anderson, W.G., Sarmiento, J.L., 2016. Mechanisms of Southern Ocean heat uptake and transport in a global eddying climate model. J. Clim. 2059–2075.
Mulvaney, R., Abram, N.J., Hindmarsh, R.C.A., Arrowsmith, C., Fleet, L., Triest, J., Sime, L.C., Alemany, O., Foord, S., 2012. Recent Antarctic Peninsula warming relative to Holocene climate and ice-shelf history. Nature 489, 141–144.
Newman, M., Alexander, M., Ault, T., Cobb, K., Deser, C., Di Lorenzo, E., Mantua, N., Miller, A., Minobe, S., Nakamura, H., Schneider, N., Vimont, D., Phillips, A., Scott, J., Smith, C., 2016. The pacific decadal oscillation, revisited. J. Clim. 29, 4399–4427.
Nürnberg, D., Böschen, T., Doering, K., Mollier-Vogel, E., Raddatz, J., Schneider, R., 2015. Sea surface and subsurface circulation dynamics off equatorial Peru during the last ~17 kyr. Paleoceanography 30, 2014PA002706.
Oppo, D.W., Rosenthal, Y., Linsley, B.K., 2009. 2,000-year-long temperature and hydrology reconstructions from the western Pacific warm pool. Nature 460, 1113–1116.
Orsi, A.J., Cornuelle, B.D., Severinghaus, J.P., 2012. Little ice age cold interval in west Antarctica: evidence from borehole temperature at the west antarctic ice sheet (WAIS) divide. Geophys. Res. Lett. 39, L09710. http://dx.doi.org/10.1029/2012GL051260.
Pahnke, K., Sachs, J.P., 2006. Sea surface temperatures of southern midlatitudes 0–160 kyr B.P. Paleoceanography 21.
Pahnke, K., Zahn, R., 2005. Southern hemisphere water mass conversion linked with North Atlantic climate variability. Science 307, 1741–1746.
Peck, V.L., Allen, C.S., Kender, S., McClymont, E.L., Hodgson, D.A., 2015. Oceanographic variability on the West Antarctic Peninsula during the Holocene and the influence of upper circumpolar deep water. Quat. Sci. Rev. 119, 54–65.
Pena, L.D., Cacho, I., Calvo, E., Pelejero, C., Eggins, S., Sadekov, A., 2008. Characterization of contaminant phases in foraminifera carbonates by electron microprobe mapping. Geochem. Geophys. Geosys. 9 http://dx.doi.org/10.1029/2008GC002018.
Pena, L.D., Goldstein, S.L., Hemming, S.R., Jones, K.M., Calvo, E., Pelejero, C., Cacho, I., 2013. Rapid changes in meridional advection of Southern Ocean intermediate waters to the tropical Pacific during the last 30 kyr. Earth Planet. Sci. Lett. 368, 20–32.
Rella, S.F., Uchida, M., 2014. A Southern Ocean trigger for northwest Pacific ventilation during the Holocene? Sci. Rep. 4, 4046.
Rhodes, R.H., Bertler, N.A.N., Baker, J.A., Steen-Larsen, H.C., Sneed, S.B., Morgenstern, U., Johnsen, S.J., 2012. Little Ice Age climate and oceanic conditions of the Ross Sea, Antarctica from a coastal ice core record. Clim. Past 8, 1223–1238.
Roemmich, D., Church, J., Gilson, J., Monselesan, D., Sutton, P., Wijffels, S., 2015. Unabated planetary warming and its ocean structure since 2006. Nat. Clim. Change 5, 240–245.
Roemmich, D., Gilson, J., Davis, R., Sutton, P., Wijffels, S., Riser, S., 2007. Decadal spinup of the south pacific subtropical gyre. J. Phys. Oceanogr. 37, 162–173.
Rosenthal, Y., Linsley, B.K., Oppo, D.W., 2013. Pacific Ocean heat content during the past 10,000 years. Science 342, 617–621.
Rosenthal, Y., Morley, A., Barras, C., Katz, M., Jorissen, F., Reichart, G.-J., Oppo, D.W., Linsley, B.K., 2011. Temperature calibration of Mg/Ca ratios in the intermediate water benthic foraminifer Hyalinea balthica. Geophys. Geochem. Geosys. 12 http://dx.doi.org/10.1029/2010GC003333.
Russell, J.L., Dixon, K.W., Gnanadesikan, A., Stouffer, R.J., Toggweiler, J.R., 2006. The southern hemisphere westerlies in a warming World: propping open the door to the deep ocean. J. Clim. 19, 6382–6390.
Schleussner, C.F., Feulner, G., 2013. A volcanically triggered regime shift in the subpolar North Atlantic Ocean as a possible origin of the Little Ice Age. Clim. Past 9, 1321–1330.
Schmidt, G.A., Jungclaus, J.H., Ammann, C.M., Bard, E., Braconnot, P., Crowley, T.J., Delaygue, G., Joos, F., Krivova, N.A., Muscheler, R., Otto-Bliesner, B.L., Pongratz, J., Shindell, D.T., Solanki, S.K., Steinhilber, F., Vieira, L.E.A., 2012. Climate forcing reconstructions for use in PMIP simulations of the Last Millennium (v1.1). Geosci. Model Dev. 5, 185–191.
Shevenell, A.E., Ingalls, A.E., Domack, E.W., Kelly, C., 2011. Holocene Southern Ocean surface temperature variability west of the antarctic peninsula. Nature 470, 250–254.
Spero, H.J., Lea, D.W., 2002. The cause of carbon isotope minimum events on glacial terminations. Science 296, 522–525.
Steig, E.J., Morse, D.L., Waddington, E.D., Stuiver, M., Grootes, P.M., Mayewski, P.A., Twickler, M.S., Whitlow, S.I., 2000. Wisconsinan and Holocene climate history from an ice core at taylor Dome, western Ross embayment, Antarctica. Geogr. Ann. Ser. A Phys. Geogr. 82, 213–235.
Stenchikov, G., Delworth, T.L., Ramaswamy, V., Stouffer, R.J., Wittenberg, A., Zeng, F., 2009. Volcanic signals in oceans. J. Geophys. Res. Atmos. 114.
Stott, L., Cannariato, K., Thunell, R., Haug, G.H., Koutavas, A., Lund, L., 2004. Decline of surface temperature an salinity in the western tropical Pacific Ocean in the Holocene epoch. Nature 431, 56–59.
Stouffer, R.J., Yin, J., Gregory, J.M., Dixon, K.W., Spelman, M.J., Hurlin, W., Weaver, A.J., Eby, M., Flato, G.M., Hasumi, H., Hu, A., Jungclaus, J.H., Kamenkovich, I.V., Levermann, A., Montoya, M., Murakami, S., Nawrath, S., Oka, A., Peltier, W.R., Robitaille, D.Y., Sokolov, A., Vettoretti, G., Weber, S.L., 2006. Investigating the causes of the response of the thermohaline circulation to past and future climate changes. J. Clim. 19, 1365–1387.
Talley, L.D., 1991. An Okhotsk Sea water anomaly: implications for ventilation in the North Pacific. Deep Sea Res. 38, 171–190.
Talley, L.D., Sprintall, J., 2005. Deep expression of the indonesian Throughflow: indonesian intermediate water in the south equatorial current. J. Geophys. Res. 110.
Thompson, D.M., Cole, J.E., Shen, G.T., Tudhope, A.W., Meehl, G.A., 2015. Early twentieth-century warming linked to tropical Pacific wind strength. Nat. Geosci. 8, 117–121.
Thompson, D.W.J., Solomon, S., Kushner, P.J., England, M.H., Grise, K.M., Karoly, D.J., 2011. Signatures of the Antarctic ozone hole in Southern Hemisphere surface climate change. Nat. Geosci. 4, 741–749.
Timmermann, A., Sachs, J., Timm, O.E., 2014. Assessing divergent SST behavior during the last 21 ka derived from alkenones and G. ruber-Mg/Ca in the equatorial Pacific. Paleoceanography 29, 680–696.
Toggweiler, J.R., Russell, J.L., Carson, S.R., 2006. Midlatitude westerlies, atmospheric $CO_2$, and climate change during the ice ages. Paleoceanography 21 n/a-n/a.
Trenberth, K.E., Fasullo, J.T., 2013. An apparent hiatus in global warming? Earths Future 1, 19–32.
Trenberth, K.E., Fasullo, J.T., Balmaseda, M.A., 2014. Earth's energy imbalance. J. Clim. 27, 3129–3144.
Tsuchiya, M., 1981. The origin of the pacific equatorial 13°C water. J. Phys. Oceanogr. 11, 794–812.
Urban, F.E., Cole, J.E., Overpeck, J.T., 2000. Influence of mean climate change on climate variability from a 155-year tropical Pacific coral record. Nature 407, 989–993.
Verleyen, E., Hodgson, D.A., Sabbe, K., Cremer, H., Emslie, S.D., Gibson, J., Hall, B., Imura, S., Kudoh, S., Marshall, G.J., McMinn, A., Melles, M., Newman, L., Roberts, D., Roberts, S.J., Singh, S.M., Sterken, M., Tavernier, I., Verkulich, S., de Vyver, E.V., Van Nieuwenhuyze, W., Wagner, B., Vyverman, W., 2011. Post-glacial regional climate variability along the East Antarctic coastal margin—evidence from shallow marine and coastal terrestrial records. Earth-Science Rev. 104, 199–212.
Woollings, T., Hoskins, B., Blackburn, M., Berrisford, P., 2008. A New rossby wave—breaking interpretation of the north atlantic oscillation. J. Atmos. Sci. 65, 609–626.
Xue, Y., Smith, T.M., Reynolds, R.W., 2003. Interdecadal changes of 30-Yr SST normals during 1871–2000. J. Clim. 16, 1601–1612.

Zenk, W., et al., 2005. Pathways and variability of the antarctic intermediate water in the western equatorial Pacific Ocean. Prog. Oceanogr. 67, 245–281.

## Acronyms

***AAIW**:* Antarctic Intermediate Water
***AMOC**:* Atlantic Meriodional Overtruning Circulation
***EEP**:* Eastern Equatorial Pacific
***EGC**:* East Greenland Current
***ENACW**:* Eastern North Atlantic Central Waters
***FTR**:* Fiji, Tonga and Rarotonga
***GHG**:* Greenhouse Gas
***HMT**:* Holocene Thermal Maximum
***ITF**:* Indonesian Throughflow
***IWT**:* intermediate water temperature
***LIA**:* Little Ice Age
***LTG**:* latitudinal temperature gradients
***MCA**:* Medieval Climate Anomaly
***NPIW**:* North Pacific Intermediate Water
***OHC**:* Ocean Heat Content
***PDO**:* Pacific Decadal Oscillation
***SAF**:* Subarctic Front
***SAMW**:* Subantarctic Mode Water
***SPG**:* Subpolar Gyre
***SPMW**:* Subpolar Mode Water
***SST**:* sea surface temperatures
***STF**:* Subtropical Front
***SWW**:* Southern Westerly Winds
***UCDW**:* Upper circumpolar Deep water
***WPWP**:* Western Pacific Warm Pool